The Journal of Experimental Biology 214, 2237-2241

doi:10.1242/jeb.055707

RESEARCH ARTICLE

Constraints on the adhesion of viscous threads spun by orb-weaving spiders: the tensile strength of glycoprotein glue exceeds its adhesion

Brent D. Opell[1,*], Harold S. Schwend[2] and Stephen T. Vito[3]

[1]Department of Biological Sciences, Virginia Tech, Blacksburg, VA 24061, USA, [2]37239 Longmoor Farm Lane, Purcellville, VA 20132, USA and [3]Department of Animal Science, University of California, One Shields Avenue, Davis, CA 95616, USA

*Author for correspondence (bopell@vt.edu)

Accepted 31 March 2011

SUMMARY

In this study we tested the hypothesis that a viscous thread releases its hold on a surface because its glycoprotein glue pulls from the surface and not because its elongating droplets break near their attachment to the surface. We compared the values obtained when three species' viscous threads adhered to four smooth surfaces, which differed in their total surface energy and in the proportions of their dispersion and polar energy components. Although water comprised 43–70% of the volume of these viscous droplets, only the dispersion surface energies of test materials and not their polar surface energies impacted thread adhesion. These results support the droplet pull-off hypothesis and are consistent with a previous finding that capillary force contributes little to thread adhesion. Just as a viscous thread's stickiness is constrained by the tensile strength of its supporting axial fibers, our findings suggest that glycoprotein adhesion is constrained by glycoprotein tensile strength.

Key words: Araneioidea, dispersion surface energy, *Leucauge venusta*, *Metepeira labyrinthea*, *Micrathena gracilis*, polar surface energy.

INTRODUCTION

The sticky viscous prey-capture threads spun by orb-weaving spiders of the Orbiculariae subclade Araneoidea are composed of regularly spaced droplets (Fig. 1), each containing a viscoelastic glycoprotein mass that confers thread adhesion (Peters, 1986; Vollrath et al., 1990; Vollrath and Tillinghast, 1991; Vollrath, 1992; Tillinghast et al., 1993; Sahni et al., 2010). These threads form the spiral component of an orb-web and are responsible for retaining insects that strike the web, providing spiders with more time to locate, run to and subdue prey before they escape (Chacón and Eberhard, 1980). Viscous threads are produced by a triad of spigots on each of a spider's paired posterior spinnerets. The single flagelliform gland spigot of this triad produces a supporting axial fiber and is flanked by two aggregate gland spigots, which coat this fiber with aqueous material (Coddington, 1989). The coated axial fibers from the two spinnerets merge to form a contiguous pair of fibers surrounded initially by a continuous sheath of viscous material. This hydrophilic material (Townley et al., 1991) absorbs atmospheric moisture soon after threads are spun in the early morning hours and condenses this moisture into a regular series of droplets (Edmonds and Vollrath, 1992), whose size and spacing differ greatly among species (Agnarsson and Blackledge, 2009; Opell and Hendricks, 2009).

Glycoprotein within each droplet confers thread adhesion (Peters, 1995; Vollrath and Tillinghast, 1991; Tillinghast et al., 1993; Opell and Hendricks, 2010). This glycoprotein adheres to a surface and, as force is applied to the thread, these viscoelastic molecules and the droplets that contain them elongate (Opell and Hendricks, 2010; Sahni et al., 2010). This allows the thread's elastic axial fibers (Blackledge and Hayashi, 2006a; Blackledge and Hayashi, 2006b) to sum adhesion from multiple droplets by implementing a suspension bridge mechanism (Opell and Hendricks, 2007; Opell et al., 2008; Opell and Hendricks, 2009). A thread's glycoprotein is encoded by the *asg1* and *asg2* genes, whose messenger RNAs are found exclusively in aggregate glands (Choresh et al., 2009). The upstream region of the 406 amino acid ASG1 protein has a high proportion of charged amino acids, which are though to be hydrophilic, and its repeating downstream region is similar to that of mucin, which is known to have adhesive properties. The upstream region of the 714 amino acid ASG2 protein is similar to known chitin-binding proteins, adapting it to adhere to insect exoskeleton, whereas its repeating downstream region has high proline content that resembles that of elastin and flagelliform spider silk, making it elastic. Thus, the properties of these proteins are consistent with the complementary adhesive, elastic and hydrophilic properties of a viscous thread's droplets.

Although we are beginning to understand how viscous threads generate adhesion, we are less certain about how their adhesion fails. Do elongating glycoprotein filaments rupture or do they pull free of a surface? At higher levels of organization, selection has favored thread release over thread rupture. The adhesion of viscous threads is always less than the tensile strength of their supporting axial fibers (Agnarsson and Blackledge, 2009), ensuring that these threads release before they break. If this functional property extends to finer levels of a thread's organization, then droplet release should result from glycoprotein pull-off rather than glycoprotein rupture.

Studies of viscous thread adhesion suggest or imply that glycoprotein pull-off is the case (Opell and Hendricks, 2007; Agnarsson and Blackledge, 2009; Opell and Hendricks, 2009). When a loaded thread is observed, it does appear to perform in this way, with outermost droplets successively elongating and releasing as force on the thread increases (Sahni et al., 2010) (T. A. Blackledge,

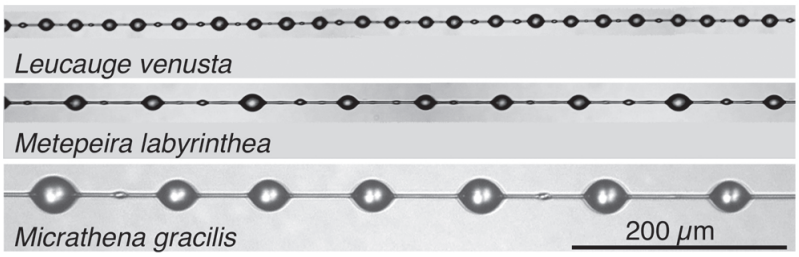

Fig. 1. Compound light microscope photographs of *Leucauge venusta, Metepeira labyrinthea* and *Micrathena gracilis* viscous threads.

personal communication; B.D.O., unpublished observations). Droplets that release from a surface reform and appear normal [fig. 8 in Opell and Hendricks (Opell and Hendricks, 2010)] and are again able to adhere to a surface and elongate when force is applied (Sahni et al., 2010) (B.D.O., unpublished observations). Moreover, a model of droplet performance that assumed glycoprotein pull-off was consistent with empirical data (Sahni et al., 2010). However, the small size of droplets leave open the possibility that the body of a contacting glycoprotein mass may separate from a thin contact layer rather than the entire mass pulling free of the surface. Indeed, studies comparing the stickiness of viscous threads note that they avoided the possibility of contamination by residues left from previously tested threads by using a new test surface or an unused portion of a test surface to measure the adhesion of each thread (e.g. Agnarsson and Blackledge, 2009; Opell and Hendricks, 2009; Sahni et al., 2010).

In this study we tested the hypothesis that a viscous thread releases its hold on a surface because its glycoprotein glue pulls from the surface and not because its elongating droplets break near their attachment to the surface. We did this by comparing the values obtained when three species' threads adhered to four smooth surfaces, which differed in their total surface energy and in the proportions of their dispersion and polar energy components. If thread release results from glycoprotein pull-off, then intraspecific differences in thread adhesion should be observed and these differences should be explained by the surface energies of the materials to which threads adhered.

MATERIALS AND METHODS

Species studied

We measured the stickiness of viscous threads spun by adult females of one member of the family Tetragnathidae, *Leucauge venusta* (Walckenaer 1842) (*N*=15), and two members of the family Araneidae, *Metepeira labyrinthea* (Hentz 1847) (*N*=11) and *Micrathena gracilis* (Walckenaer 1842) (*N*=12), all collected within 10 km of Blacksburg, Montgomery County, VA, USA. *Leucauge venusta* built webs less than 1 m above the ground near forest edges or in other partially shaded, moist habitats. *Metepeira labyrinthea* occupied dryer, more exposed habitats, where they built webs 1–2 m above the ground. *Micrathena gracilis* constructed their webs 1–2 m above the floor of moist forests. The droplet sizes, spacing and percent moisture composition of these species differed, as reported in the literature (Opell and Hendricks, 2009) and summarized in Table 1. In the context of temperate orb-weaving spiders, these three species have medium to small viscous droplets (Agnarsson and Blackledge, 2009; Opell and Hendricks, 2009).

Collecting threads and measuring thread stickiness

Following techniques described previously (Opell and Hendricks, 2009), we collected orb-web samples on 17 cm diameter rings with Scotch® double-coated tissue tape (tape 4101T; 3M, St Paul, MN, USA) applied to their 5 mm wide rims to maintain threads at their native tensions. Threads from the outer third of orb-webs were sub-sampled on 4.8 mm square brass bars glued at 4.8 mm spacing to a microscope slide. Double-sided Scotch® tape (tape 665; 3M) on the upper surfaces of these supports held threads at their native tensions. After removing alternate spiral turns to prevent the contact plate used to measure stickiness from contacting multiple threads, we examined threads under a dissecting microscope to ensure that they were intact. The microscope slide thread sampler was then clamped to a mechanism that pressed a thread against the contact plate at a constant speed of 0.06 mm s^{-1} until a force of 25.0 μN was exerted on the plate, at which time the direction of travel was immediately reversed, pulling the thread away from the contact plate at the same speed until the two separated. This 1891 μm wide (s.d.=22 μm, *N*=16) contact plate was attached to the lever arm of a load cell, enabling the maximum force registered before thread release to be observed and recorded.

On the day that an individual spider's threads were collected, we measured the stickiness of thread strands with contact plates

Table 1. Features of the three study species' primary viscous droplets [from Opell and Hendricks (Opell and Hendricks, 2009)], the number of droplets per contact plate width used in the present study to measure thread adhesion, the grand mean adhesion per droplet based on this droplet number and the conditions under which thread adhesion was measured

	Leucauge venusta	*Micrathena gracilis*	*Metepeira labyrinthea*
Droplet features			
% Water	70	43	66
Droplet length (μm)	13.8	30.2	23.5
Droplet width (μm)	10.0	23.5	16.4
Droplet volume (μm^3)	698	7510	3014
Droplets per mm	29.9	9.9	17.5
Droplets per plate	56.5	18.7	33.1
Grand mean adhesion per droplet (μN; ±1 s.e.m.)	1.500±0.068	3.942±0.154	3.596±0.116
Test conditions			
Temperature (°C)	24.0±0.02	24.0±0.00	24.0±0.00
% Relative humidity	43.9±0.5	45.5±0.3	44.9±0.3

Table 2. Physical properties of water and 1-bromonaphthalene test liquids at 20°C [from Rathod and Hatzikiriakos (Rathod and Hatzikiriakos, 2004)]

	Water	1-Bromonaphthalene
Surface energy: Υ_L (mJ m^{-2})	72.6	44.6
Surface energy from London dispersion forces: Υ_L^D (mJ m^{-2})	21.6	44.6
Surface energy from hydrogen bonding: Υ_L^P (mJ m^{-2})	51.0	0

surfaced with each of the four test materials within the same 1 h period. The 5 mm length of a contact plate allowed us to measure the stickiness of three strands before replacing its surface to ensure that a thread strand always contacted an unused region of the surface. The three measurements taken with each surface were averaged to produce a set of four stickiness values per individual spider.

Determining the surface energies of the four surfaces

The four test materials we used were: CS Hyde® Optically clear polytetrafluoroethylene (PTFE) (Teflon) FEP tape with silicone adhesive backing for the PTFE surface, Glad Cling Wrap® for the low-density polyethylene (LDPE) surface, Scotch Magic® tape (tape 810; 3M) for the acetate surface, and the shiny surface of Reynolds Wrap® aluminium foil for the aluminium surface. Material of each type was taken from the same roll or package to ensure consistency. All contact plate surfaces were prepared by the same individual to ensure consistency. As the formulation of these materials can differ and as it has long been known that the surface texture of a material affects its expressed surface energy (Wenzel, 1936), rather than using generic surface energy values we determined the dispersion (non-polar) surface energy (Υ_S^D; mJ m^{-2}) and polar surface energy (Υ_S^P) components of the surface energy (Υ_S) of each material following the methods described by Rathod and Hatzikiriakos (Rathod and Hatzikiriakos, 2004). We did this by measuring the contact angles of 5 µl droplets of water (HPLC/spectrophotometry grade Optima Water, Fisher, Pittsburgh, PA, USA) and 1-bromonaphthalene 96% (MDL no. MFCD00003868, Acros Organics, Fair Lawn, NJ, USA) that were placed onto each material using an Eppendorf® 10 µl micropipette. To achieve this we photographed droplets with a dissecting microscope on whose stage we positioned a front-surfaced, right-angle prism mounted to a plate that held a microscope slide to which the surface being evaluated was affixed (Fig. 2). These images were taken at a temperature of 21°C, which was the closest constant temperature to the 20°C standard for which the surfaces energies of the test liquids were reported (Table 2) that we could establish. Each of us used Image J (Rasband, 1997-2011) to measure the contact angle on each edge of a droplet independently and averaged these six values to obtain the contact angles shown in Table 3.

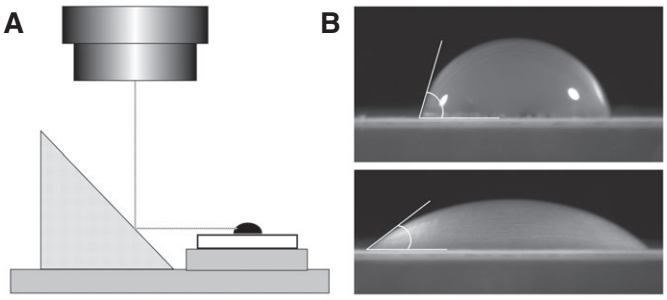

Fig. 2. (A) Diagram of the method used to photograph drops on the test surfaces and (B) photographs of water (upper) and 1-bromonaphthalene (lower) drops on an acetate surface, showing their contact angles.

Using the values reported in Tables 2 and 3, we solved the unknown values Υ_S^D and Υ_S^P in the following equation:

$$1 + \cos\theta = 2 / \Upsilon_L \{[\sqrt{(\Upsilon_S^D \times \Upsilon_L^D)}] + [\sqrt{(\Upsilon_S^P \times \Upsilon_L^P)}]\}, \quad (1)$$

where $\cos\theta$ is the measured contact angle, Υ_L is the surface energy of the test liquid, Υ_L^D is the non-polar surface energy of the test liquid and Υ_L^P is the polar surface energy of the test liquid. We solved the equation first for values of 1-bromonaphthalene, as its Υ_L^P value of 0 causes the polar (right) side of the equation to be 0 and provides a test surface's Υ_S^D that was then used in solving the equation for the values of water. Fig. 3 presents the results of these computations.

Statistical analyses

We used the JPM statistical analysis program (SAS Institute, Cary, NC, USA) to analyze data, considering $P \leq 0.05$ to be significant.

RESULTS

A comparison of our four surface energy values with those reported in the literature shows that our values are appropriate and confirms the usefulness of determining these values rather than using nominal values. For acetate, our 38.2 mJ m^{-2} is identical to the reported value (Busscher and Arends, 1981). The reported 42.9 mJ m^{-2} of aluminium (Hansen et al., 1993) corresponds well with our 45.4 mJ m^{-2}, obtained when we averaged the 38.8 mJ m^{-2} measured on the dull side of aluminium foil and the 51.9 mJ m^{-2} that we measured on the shiny side of the foil. Our 50.5 mJ m^{-2} for the LDPE in Glad Cling Wrap® is greater that the 33 mJ m^{-2} reported for polyethylene (Bezigian, 1992). However, to improve its adherence to containers, the surface energy of plastic food wrap film is typically increased by methods such as corona discharge treatment (Mangipudi and Tirrell, 1996). This process alters the film's surface properties and 'as polar groups are introduced on the surface, the surface energy of PE can increase from about 33 to 55 mJ m^{-2}' (Mangipudi and Tirrell, 1996). Other procedures, such as low pressure O_2 plasma treatment, can produce LDPE with surface energies as high as 69 mJ m^{-2} (Sanchis et al., 2006). Consequently, we believe that our values are accurate. Finally, our Teflon value of 27.4 mJ m^{-2} is greater than the reported 24 mJ m^{-2} (Good, 1964), although, as expected, it was the lowest of the four values. We used

Table 3. Contact angles (deg) of the four surfaces used to measure thread stickiness

	Water	1-Bromonaphthalene
PTFE	91.29±2.215	61.49±3.80
Acetate	79.95±5.209	43.20±4.29
LDPE	64.47±2.76	24.26±2.94
Aluminium	56.25±3.60	37.53±2.17

Data are means ±1 s.e.m. of measurement precision.

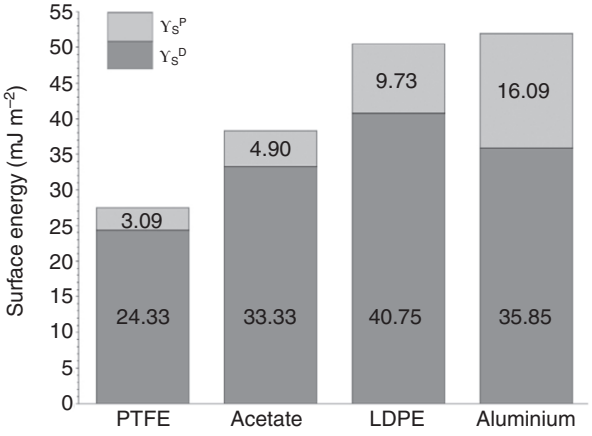

Fig. 3. The total surface energy of the four test materials and their polar and dispersion components. LDPE, low-density polyethylene; PTFE, polytetrafluoroethylene.

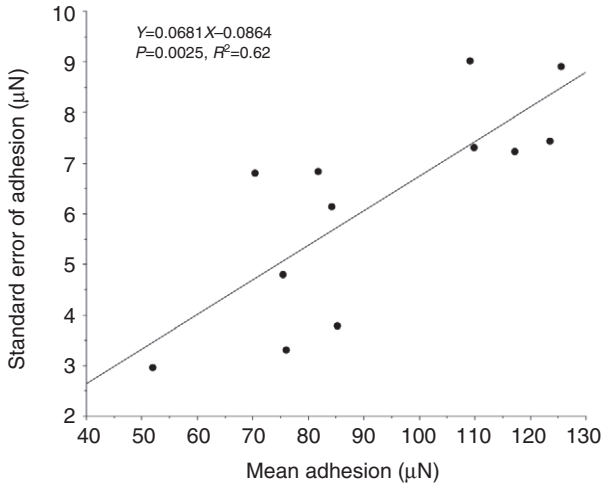

Fig. 5. The relationship between the mean adhesion of each species' threads on the four test surfaces and the standard errors of these means.

Teflon tape that had an applied adhesive backing. When this tape was dispensed from a roll, the adhesive backing of one layer released freely from the exposed Teflon of the underling layer. However, it is possible that when this occurred the exposed Teflon surface was altered in a manner similar to that described above for polyethylene.

Thread adhesion differed both among species and among test surfaces (Fig. 4), despite the tendency for measurement error to increase as adhesion increased (Fig. 5). An ANOVA documented interspecific differences in thread stickiness and showed that the small differences in the relative humidity (RH) and temperature at which stickiness was measured did not contribute to this difference (model, P=0.0001; species, P=0.0001; RH, P=0.2734; temperature, P=0.2459), an observation that is consistent with earlier findings (Opell and Hendricks, 2009). The grand mean (±s.e.m.) adhesion of *M. labyrinthea* (119.04±3.85 μN) is 1.404 times that of *L. venusta* (84.77±3.86 μN) and 1.615 times that of *M. gracilis* (73.72±2.88 μN). Multiplying the adhesion values of *L. venusta* and *M. gracilis* by their respective indices standardizes adhesion across the three species. This is verified by a two-factor ANOVA, which examines the effects of species and test surface on standardized thread adhesion (model, P=0.0001; species, P=1.000; test material, P=0.0001). An ANOVA that included species, γ_S^D and γ_S^P was also significant, but with species and γ_S^P failing to contribute to standardized adhesion (model, P=0.0001; species, P=1.000; γ_S^D, P=0.0001; γ_S^P, P=0.5369).

A regression of the three species' mean standardized adhesive values against the γ_S^D values of the four test surfaces provides further support for the impact of surface energy on thread stickiness (Fig. 6). We attempted to document that the γ_S^P values of the four test surfaces made a small contribution to thread adhesion by examining their relationship to the regression residuals of the 12 standardized stickiness values shown in Fig. 6, but found no

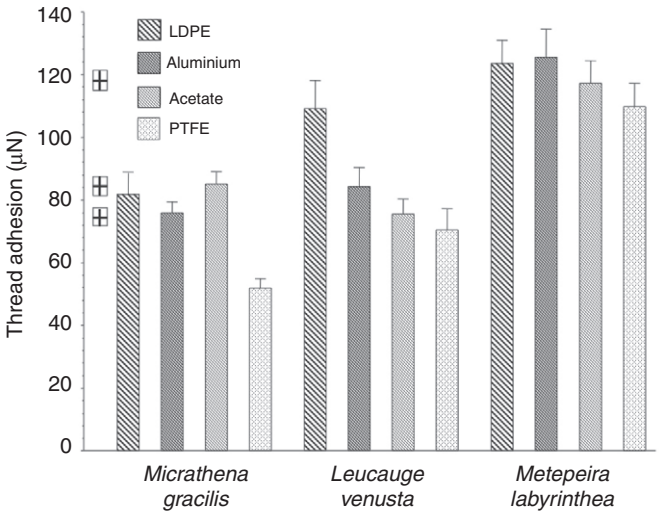

Fig. 4. Histogram of the adhesion of the three species' threads on each of the four test surfaces. Error bars represent ±s.e.m. Horizontal lines in the box plots on the left edge indicate the grand mean adhesion of, from bottom to top, *M. gracilis*, *L. venusta* and *M. labyrinthea*, and heights of these boxes correspond to the standard errors of these means.

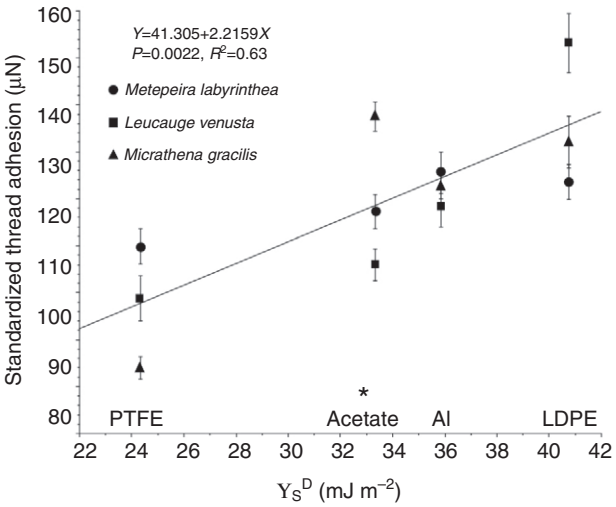

Fig. 6. Regression of the three species' mean standardized adhesion values on the dispersion surface energies of the four test surfaces. To minimize overlap, error bars represent ±0.5 s.e.m. The asterisk indicates a significant difference among species.

relationship (P=0.9576). *Metepeira labyrinthea* threads appear to exhibit the greatest adhesion on PTFE and aluminium, *M. gracilis* threads the greatest values on acetate, and *L. venusta* threads the greatest values on LDPE. However, the apparent disparity in this ranking of the species' values has little meaning, as surface-by-surface ANOVAs document significant interspecific differences in standardized adhesion only on acetate surfaces (P=0.0067). On this surface, the order of these standardized adhesive values (from high to low: *M. gracilis*, *M. labyrinthea* and *L. venusta*) corresponds directly to the grand mean stickiness per droplet of these species (Table 1), suggesting that differences in droplet spacing contribute to interspecific differences in standardized thread stickiness.

DISCUSSION

Our finding that dispersion surface energy affected thread adhesion, combined with the results of a recent study of droplet performance (Sahni et al., 2010), provides convincing support for the hypothesis that threads release their hold on surfaces because glycoprotein pulls from the surface, not because it breaks or splits at its attachment to the surface. This conclusion suggests that, just as a viscous thread's stickiness is constrained by the tensile strength of its axial fibers (Agnarsson and Blackledge, 2009), the adhesion of a thread's glycoprotein is constrained by its tensile strength. We would expect the polar component of a surface's energy to interact with the water in viscous thread droplets. Therefore, our failure to document a significant contribution of γ_S^P to thread adhesion, despite differences in γ_S^P, the proportion of the test surfaces' γ_S^D and γ_S^P values, and the water content of the three species' droplets, is consistent with the finding that glycoprotein adhesion is much greater than the capillary forces resulting from water within thread droplets (Sahni et al., 2010).

ACKNOWLEDGEMENTS

This study was supported by National Science Foundation grant IOB-0445137. Mary L. Hendricks assisted with data analysis.

REFERENCES

Agnarsson, I. and Blackledge, T. A. (2009). Can a spider web be too sticky? Tensile mechanics constrains the evolution of capture spiral stickiness in orb weaving spiders. *J. Zool.* **278**, 134-140.

Bezigian, T. (1992). The effect of corona discharge onto polymer films. *Tappi J.* **75**, 139-141.

Blackledge, T. A. and Hayashi, C. Y. (2006a). Silken toolkits: biomechanics of silk fibers spun by the orb web spider *Argiope argentata* (Fabricius 1775). *J. Exp. Biol.* **209**, 2452-2461.

Blackledge, T. A. and Hayashi, C. Y. (2006b). Unraveling the mechanical properties of composite silk threads spun by cribellate orbweaving spiders. *J. Exp. Biol.* **209**, 3131-3140.

Busscher, H. J. and Arends, J. (1981). Determination of the dispersion and polar surface forces from contact angle measurements on polymers and dental enamel. *J Col. Inter. Sci.* **81**, 75-79.

Chacón, P. and Eberhard, W. G. (1980). Factors affecting numbers and kinds of prey caught in artificial spider webs with considerations of how orb-webs trap prey. *Bull. Br. Arachnol. Soc.* **5**, 29-38.

Choresh, O., Bayarmagnai, B. and Lewis, R. V. (2009). Spider web glue: two proteins expressed from opposite strands of the same DNA sequence. *Biomacromolecules* **10**, 2852-2856.

Coddington, J. A. (1989). Spinneret silk spigot morphology: evidence for the monophyly of orb-weaving spiders, Cyrtophorinae (Araneidae), and the group Theridiidae plus Nesticidae. *J. Arachnol.* **17**, 71-96.

Edmonds, D. and Vollrath, F. (1992). The contribution of atmospheric water vapour to the formation and efficiency of a spider's web. *Proc. R. Soc. Lond.* **248**, 145-148.

Good, R. J. (1964). Theory for the estimation of surface and interfacial energies VI. Surface energies of some flurocarbon surfaces from contact angle measurements. In *Contact Angle, Wettability and Adhesion* (ed. F. M. Fowkes), pp. 74-87. Washington, DC: American Chemical Society.

Hansen, M. H., Finlayson, M. F., Castille, M. J. and Goins, J. D. (1993). The role of corona discharge treatment in improving polyethylene-aluminum adhesion: an acid-base perspective. *Tappi J.* **76**, 171-177.

Mangipudi, V. and Tirrell, M. (1996). Direct measurement of the surface energy of corona-treated polyethylene using the surface forces apparatus. *Langmuir* **11**, 19-23.

Opell, B. D. and Hendricks, M. L. (2007). Adhesive recruitment by the viscous capture threads of araneoid orb-weaving spiders. *J. Exp. Biol.* **210**, 553-560.

Opell, B. D. and Hendricks, M. L. (2009). The adhesive delivery system of viscous prey capture threads spin by orb-weaving spiders. *J. Exp. Biol.* **212**, 3026-3034.

Opell, B. D. and Hendricks, M. L. (2010). The role of granules within viscous capture threads of orb-weaving spiders. *J. Exp. Biol.* **212**, 3026-3034.

Opell, B. D., Markley, B. J., Hannum, C. D. and Hendricks, M. L. (2008). The contribution of axial fiber extensibility to the adhesion of viscous capture threads spun by orb-weaving spiders. *J. Exp. Biol.* **211**, 2243-2251.

Peters, H. M. (1986). Fine structure and function of capture threads. In *Ecophysiology of Spiders* (ed. W. Nentwig), pp. 187-202. New York: Springer Verlag.

Peters, H. M. (1995). Ultrastructure of orb spiders' gluey capture threads. *Naturwissenschaften* **82**, 380-382.

Rasband, W. S. (1997-2011). ImageJ, US National Institutes of Health, Bethesda, MD, USA, http://imagej.nih.gov/ij/.

Rathod, N. and Hatzikiriakos, S. G. (2004). The effect of surface energy of boron nitride on polymer processability. *Polymer Eng. Sci.* **44**, 1543-1550.

Sahni, V., Blackledge, T. A. and Dhinojwala, A. (2010). Viscoelastic solids explain spider web stickiness. *Nat. Commun.* **1**, doi:10.1038/ncomms1019.

Sanchis, M. R., Blanes, V., Blanes, M., Garcia, D. and Balart, R. (2006). Surface modification of low-density polyethylene (LDPE) film by low pressure O_2 plasma treatment. *Eur. Polymer J.* **42**, 1558-1568.

Tillinghast, E. K., Townley, M. A., Wight, T. N., Uhlenbruck, G. and Janssen, E. (1993). The adhesive glycoprotein of the orb web of *Argiope aurantia* (Araneae, Araneidae). *Mat. Res. Soc. Symp. Proc.* **292**, 9-23.

Townley, M. A., Bernstein, D. T., Gallagher, K. S. and Tillinghast, E. K. (1991). Comparative study of orb-web hydroscopicity and adhesive spiral composition in three areneid spiders. *J. Exp. Zool.* **259**, 154-165.

Vollrath, F. (1992). Spider webs and silks. *Sci. Am.* **266**, 70-76.

Vollrath, F. and Tillinghast, E. K. (1991). Glycoprotein glue beneath a spider web's aqueous coat. *Naturwissenschaften* **78**, 557-559.

Vollrath, F., Fairbrother, W. J., Williams, R. J. P., Tillinghast, E. K., Bernstein, D. T., Gallagher, K. S. and Townley, M. A. (1990). Compounds in the droplets of the orb spider's viscid spiral. *Nature* **345**, 526-528.

Wenzel, R. N. (1936). Resistance of solid surfaces to wetting by water. *Ind. Eng. Chem.* **28**, 988-994.